

1 Supplementary Material to “Do terrestrial hermit crabs sniff?”

2 Air flow and odorant capture by flicking antennules”

3 Lindsay D. Waldrop*^{1,2} and M. A. R. Koehl²

4 ¹*Author of Correspondence. Current address: School of Natural Sciences, Univ. of

5 California, Merced, USA. Email: lwaldrop@ucmerced.edu

6 ²Dept. of Integrative Biology, Univ. of California, Berkeley, CA, USA

7 November 30, 2015

8 **Abstract**

9 Supplementary material accompanying the paper “Do terrestrial hermit crabs sniff? Air flow
10 and odorant capture by flicking antennules.” Includes details of the computational model simulating
11 odor transport to the chemosensory hairs based on PIV data.

12 **Keywords:** olfaction, hermit crab, fluid dynamics, aesthetasc, flicking

13 **Markov-Chain Monte Carlo Computational Model**

14 We simulated the transport of odorant molecules to the ventral surfaces of aesthetascs on an antennule
15 of *C. rugosus*, using a 2D Markov-chain Monte Carlo simulation. To simulate convection during flicks,

16 we used our PIV data in air with a finite-difference, forward-Euler approximation, and to simulate
17 diffusion, we used two, 1D random walks of odorant molecules. All simulations were performed in
18 Matlab (R2014a). The flick was divided into n time steps with duration $\Delta t = 7.82 \times 10^{-6}$ s. For each
19 time step, the position $P(X, Y)$ of each odour molecule was advanced using a finite-difference, forward
20 Euler approximation based on PIV velocity vector fields:

$$21 \quad X(t + 1/2\Delta t) = X(t) + u(X(t))\Delta t \quad (1)$$

$$22 \quad Y(t + 1/2\Delta t) = Y(t) + v(Y(t))\Delta t \quad (2)$$

23 Eqn. 1 uses u for the X component of position and Eq. 2 uses v for the Y component of position.

24 Diffusion for each time step was advanced based on the root mean squared distance of diffusion

25 ($L_{RMS} = \sqrt{2D\Delta t}$) to yield the equations:

$$26 \quad X(t + \Delta t) = X(t + 1/2\Delta t) + i\sqrt{D\Delta t} \quad (3)$$

$$27 \quad Y(t + \Delta t) = Y(t + 1/2\Delta t) + i\sqrt{D\Delta t} \quad (4)$$

28 where i was assigned the values -1, 0, or +1 based on Matlab's pseudorandom number generator for
29 each component of position independently.

30 A patch of 100,000 simulated odorant molecules (M_{total}) was created over an area of 3.48×10^{-10}
31 m^2 (see Fig. 1); odorant molecules were evenly spaced along each axis within the area. The density of
32 simulated odorant molecules corresponds to a concentration of 0.46 parts per billion of caproic acid in
33 air based on mass.

34 We assumed that the aesthetasc array was a perfect absorber, so that any odor molecules that crossed
35 the boundary line were removed from the fluid and counted as captured at each time step. The total
36 number of molecules captured was divided by the starting number of molecules to find the percent total
37 molecules captured, M . The location of the outer boundary of the physical model's aesthetasc array
38 was chosen from raw data images (shown in Fig. 1, all panels).

39 Since we used measured PIV velocity vector fields, there was the possibility that non-zero velocity
40 vectors could exist close to or on the boundary of each aesthetasc due to measurement error, which
41 would be a violation of the no-slip condition. We verified that there was no violation of the no-slip
42 condition by running a simulation in which diffusion coefficient D was set to 0 (no diffusion case); the
43 no-diffusion case captured no molecules during an entire downstroke-return stroke event, indicating
44 that either the no-slip condition is not violated or that the violations were so small that they did not
45 inflate the capture of simulated molecules.

46 Another assumption of our computational was that the velocity vector field was divergence-free,
47 an indication that there is no flow in the dimension normal to the plan in which we measured veloci-
48 ties. Divergence is relatively low, except at position values very close to the edge of the plot (Fig. 2,
49 high X -position values). Since these are 2D velocity vector fields sampled from a 3D velocity vector
50 field, divergence in 2D fields is expected. In other models, 2D velocity vector fields were decomposed
51 to create non-unique solutions of divergence and divergence-free velocity fields which differ from the
52 measured fields [1], but we have chosen to rely on raw PIV data from the model without this decompo-
53 sition in order to stay true to fluid flow around the model.

54 **Convergence Testing**

55 To determine the time-step used for simulations, simulations were run using numbers of steps ranging
56 from 100 to 20,000 with 100,000 simulated molecules with $D = 6 \times 10^{-6} \text{ m}^2 \text{ s}^{-1}$ for three repetitions
57 (Fig. 3A). Convergence on a final number of molecules per total molecules captured was observed at
58 around 8.8%. The number of steps reaching very close (within the standard deviation of three runs) by
59 10,000 time steps, so this number ($\Delta t = 7.82 \times 10^{-6} \text{ s}$) was chosen for all runs with diffusivities.

60 Convergence in concentration was tested by varying M_{total} within the initial starting area between
61 2,500 and 12.3 million simulated molecules, corresponding roughly to concentrations of 0.0012 to 5.65
62 ppb in air (Fig. 3B). Three repetitions of these conditions revealed that the per-cent of total molecules
63 captured had no dependence on initial concentration, but higher standard deviations were observed for
64 concentrations under 0.4615 ppb (100,000 simulated molecules), so a concentration of 0.46 ppb was
65 used for simulations unless otherwise noted.

66 **Data Archiving**

67 All data are available at FigShare: <http://dx.doi.org/10.6084/m9.figshare.1558300>.

68 **References**

69 [1] Stacey, M., Mead, K. & Koehl, M., 2002 Molecule capture by olfactory antennules: Mantis shrimp.

70 *J. Math. Biol.* **44**, 1–30.

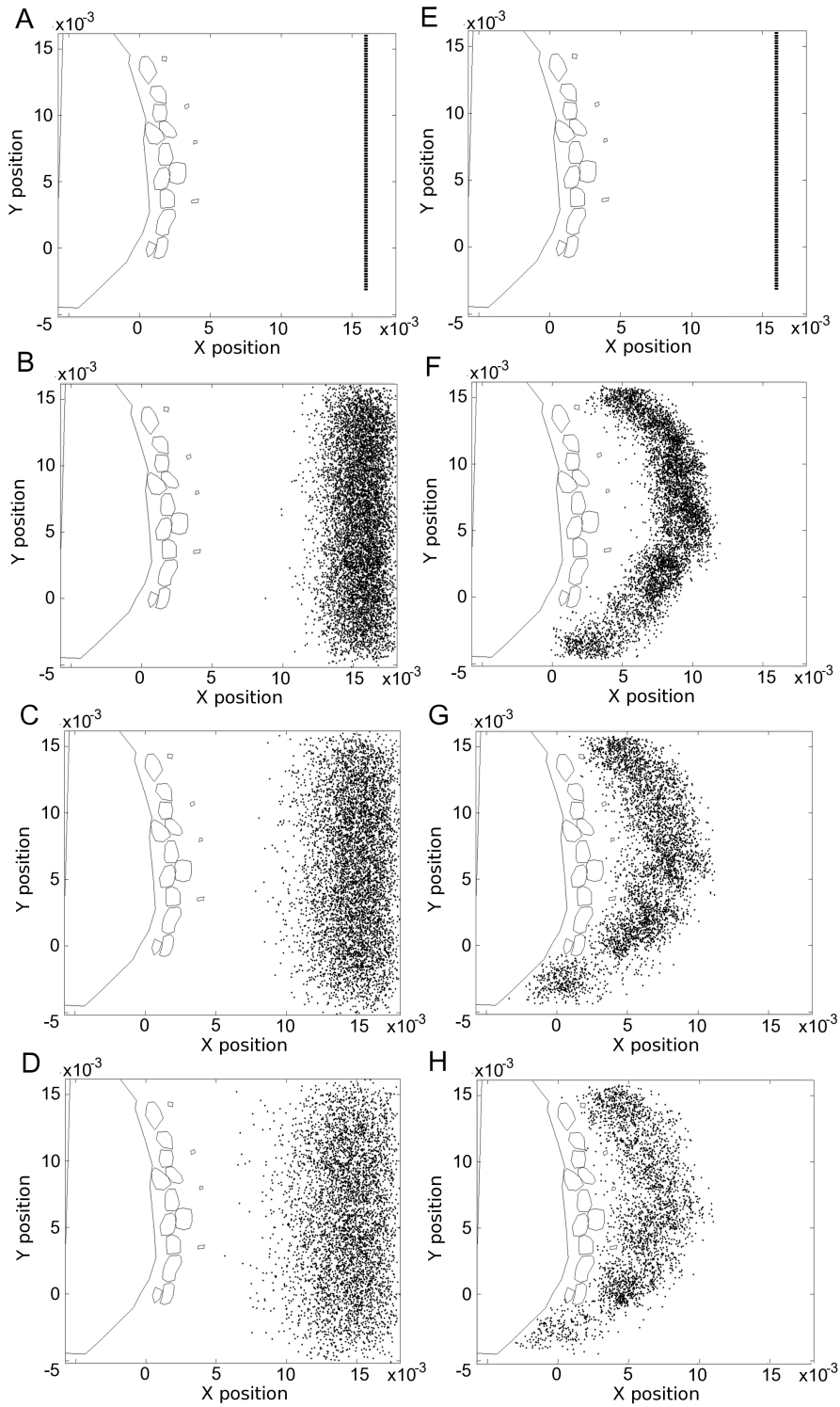


Figure 1 (*preceding page*): Computational model of odor transport based on grid established during particle image velocimetry at $D = 5 \times 10^{-8} \text{ m}^2 \text{ s}^{-1}$ for two simulation conditions: still antennule (A-D) and flicking antennule (E-H). Position of the flagellum and aesthetascs marked with black lines. The positions of simulated odor molecules are plotted at times 0 s (initial positions; A,E), 7.82 ms (B,F), 15.6 ms (C,G), and 23.5 ms (D,H).

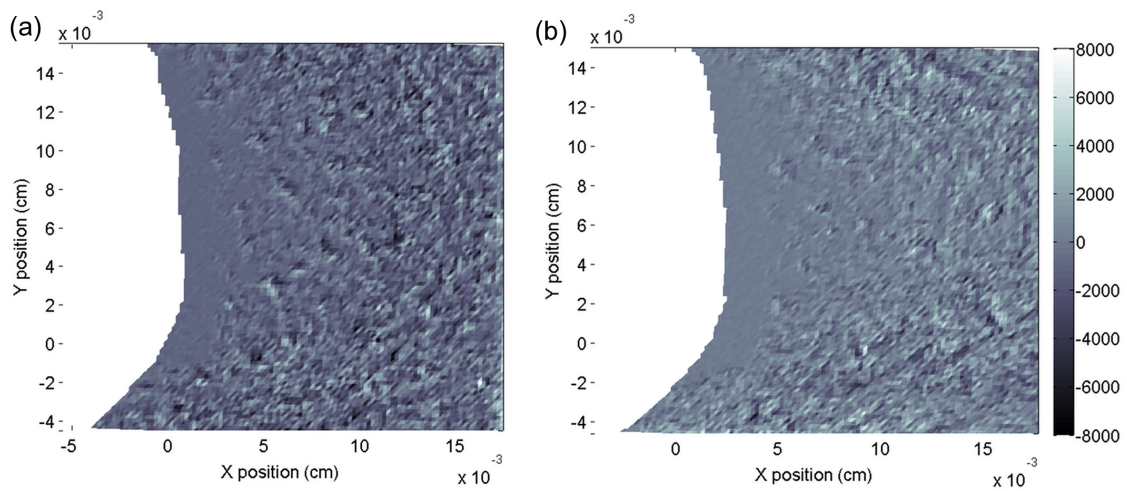


Figure 2: Divergence of the downstroke (a) and return stroke (b) PIV velocity vector fields used for the computational model.

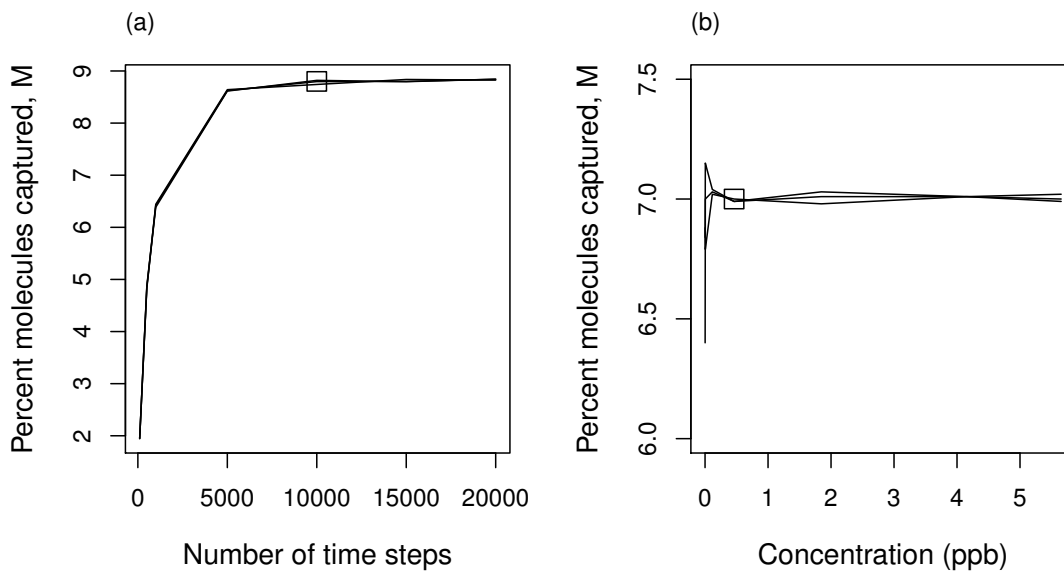


Figure 3: Convergence testing plots for diffusivities in air ($D = 6.02 \times 10^{-6} \text{ m}^2 \text{ s}^{-1}$). Each plot contains three replicate simulations at each point. Square boxes indicate chosen parameters for regular simulations. A: Temporal. Percentage of total odor molecules captured versus number of time steps that the flick duration was divided. B: Concentration. Percentage of total odor molecules captured versus initial concentration of odor patch in parts per billion (ppb).